Journal of MATERIALS RESEARCH

Invited Paper
DOI: 10.1557/jmr.2019.143

FOCUS ISSUE

THERMODYNAMICS OF COMPLEX SOLIDS

Enthalpy increments and redox thermodynamics of $SrFeO_{3-\delta}$

Vladimir Sereda[1,a], Anton Sednev[1], Dmitry Tsvetkov[2], Andrey Zuev[2]

[1]Department of Physical and Inorganic Chemistry, Institute of Natural Sciences and Mathematics, Ural Federal University, Yekaterinburg 620002, Russia; and Department of Solid State Electrochemistry, Institute of High-Temperature Electrochemistry UB RAS, Yekaterinburg 620137, Russia
[2]Department of Physical and Inorganic Chemistry, Institute of Natural Sciences and Mathematics, Ural Federal University, Yekaterinburg 620002, Russia

[a]Address all correspondence to this author. e-mail: vladimir.sereda@urfu.ru

Received: 11 January 2019; accepted: 27 March 2019

Enthalpy increments, $\Delta_{298}^{T}H^{0}$, for highly nonstoichiometric $SrFeO_{3-\delta}$ (δ = 0.18–0.41) were obtained between 373 and 1273 K in air using drop calorimetry. The analysis of the $\Delta_{298}^{T}H^{0}(T)$ dependence at lower temperatures allowed evaluating the enthalpy of tetragonal to cubic $I4/mmm \rightarrow Pm\bar{3}m$ phase transition at 560 K, 1.57 kJ/mol, and the Maier–Kelley function for $\Delta_{298}^{T}H^{0}(T)$ of tetragonal $SrFeO_{3-\delta}$ (space group $I4/mmm$). Combined investigation of oxygen nonstoichiometry $\delta(T)$ dependence, measured by thermogravimetry, and higher-temperature $\Delta_{298}^{T}H^{0}(T)$ of cubic $SrFeO_{3-\delta}$ (space group $Pm\bar{3}m$) yielded the temperature-dependent reduction (oxygen release) enthalpy, ΔH_{red}^{0}. Calorimetrically-determined ΔH_{red}^{0} of $SrFeO_{3-\delta}$ increases from 65 ± 7 kJ/mol O at 873–973 K to 84 ± 7 kJ/mol O at 1073–1273 K, which may indicate that the short-range vacancy ordering in $SrFeO_{3-\delta}$ is hampered at higher temperatures.

Introduction

Structure and properties of undoped strontium ferrite $SrFeO_{3-\delta}$ (SF) have been the focus of numerous scientific investigations over the last several decades. This oxide is stable over the wide range of oxygen content, from $(3-\delta) = 2.5$ to 3.0. The oxygen nonstoichiometry (δ) in SF is governed by the equilibrium temperature (T) and oxygen partial pressure (p_{O_2}). It is known that various ordered phases with different δ, such as $Sr_8Fe_8O_{23}$ (space group $I4/mmm$), $Sr_4Fe_4O_{11}$ ($Cmmm$) and $Sr_2Fe_2O_5$ ($Ibm2$), can be formed in SF system depending on the particular T and p_{O_2} [1, 2, 3, 4]. However, such ordered phases and their transformations are interesting mainly from the fundamental point of view. It can be said that the disordered-cubic-perovskite-like structure ($Pm\bar{3}m$) is the most important for the practical applications because its stability limits with respect to T and p_{O_2} overlap the working conditions of many state-of-the-art electrochemical devices including solid oxide fuel cells (SOFC) and oxygen permeation membranes [5, 6]. Additionally, the number of publications on substituted SF ($Sr_{1-x}A_xFe_{1-y}B_yO_{3-\delta}$ where A is a rare-earth metal and B—3d-transition metal) grows steadily—and such substitutions are usually aimed not only at enhancing the properties of the parent compound, but also at stabilizing its perovskite-type structure.

A lot of potential high-temperature applications of perovskite-type oxides, such as sensors, membranes and SOFC components, are related to the oxygen exchange phenomena. Understanding the redox energetics could provide useful insights into the defect chemistry [7] and even the microstructure [8] of the oxide in question. In this regard, an extensive calorimetric study of different phases in SF system was made by Haavik et al. [9, 10, 11]. However, their direct heat capacity (C_p) measurements on cubic $SrFeO_{2.83}$ were made only up to around 700 K [11], where little oxygen exchange of this sample with ambient atmosphere (air) actually occurs. In the paper on enthalpy contribution to the redox thermodynamics of SF [10] they report temperature-dependent oxidation enthalpies, ΔH_{ox}^{0}, of perovskite-type SF for T in range 800–1200 K. Lacking the actual high-temperature experimental data, rather questionable procedure was employed for obtaining these dependences. Two-phase samples with general formula $SrFeO_{2.54}$, consisting of brownmillerite-type $Sr_2Fe_2O_5$ with unknown amount of $Sr_4Fe_4O_{11}$-type impurity, were taken as initial (reduced) strontium ferrite. Then these samples were heated in air in the

https://doi.org/10.1557/jmr.2019.143 Published online by Cambridge University Press

© Materials Research Society 2019

adiabatic calorimeter up to approximately 700 K, resulting in their oxidation at around 600 K accompanied by transformation into cubic SF and corresponding heat effects. The oxygen content in resulting oxide was found to be close to 2.83. Strictly speaking, in order to calculate the high-temperature heats of oxidation of perovskite-type SF using the results of such experiment, a lot of additional reliable data are needed: the quantitative phase composition of initial $SrFeO_{2.54}$ oxides, the heats of $Ibm2 \rightarrow Pm\bar{3}m$ and $Cmmm \rightarrow Pm\bar{3}m$ phase transitions, and the enthalpy increments of all the phases in question. In fact, Haavik et al. [10] neglected the impurities in reduced SF, assuming that $SrFeO_{2.54}$ consisted of single-phase brownmillerite. The values of order-disorder $Ibm2 \rightarrow Pm\bar{3}m$ transition enthalpy in $SrFeO_{2.5}$, used in calculations by Haavik et al. [10], differed by 2.5 kJ/mol oxide. This led to the additional ambiguity in the reported ΔH^0_{ox} of 7.5 kJ/mol O, which is comparable to the uncertainty of their calorimetric measurements. Moreover, the enthalpy increments for orthorhombic $SrFeO_{2.5}$ and cubic $SrFeO_{2.83}$ were calculated using extrapolated and not experimental $C_p(T)$ dependences [9]. The said extrapolation was done on the basis of Neumann–Kopp rule. As the lattice-dynamic behavior is expected to be quite different for $SrFeO_{2.5}$, $SrFeO_{2.83}$, SrO, and Fe_2O_3 if only because their crystal structure differs significantly, Neumann–Kopp rule is expected to give erroneous temperature dependences of specific heat of either $SrFeO_{2.5}$ or $SrFeO_{2.83}$.

Cheng et al. [8] reported ΔH^0_{ox} of SF to be -70 ± 15 kJ/mol O. Though this value is extrapolated from compositional dependences, $\Delta H^0_{ox}(La_{1-x}Sr_xFeO_{3-\delta}) = f(x)$, the values of ΔH^0_{ox} reported by Cheng et al. [8] and Haavik et al. [10] are well within the error margins of each other.

The recent ab initio calculations of heat capacity of SF made by Jia et al. [12] differ from the experimental results [11] in almost all aspects—from the absence of any signs of phase transitions on $C_p(T)$ dependences to the C_p values.

Several studies reported equilibrium oxygen partial pressure–composition–temperature ($p_{O_2} - T - \delta$) data for SF [2, 7, 13, 14, 15, 16, 17, 18, 19, 20]. These data can be used to calculate partial molar enthalpy, Δh_O, and entropy, Δs_O, of oxygen according to the well-known relations. Existing significant scatter in published $p_{O_2} - T - \delta$ data [10] inevitably leads to considerable discrepancies in as-estimated partial molar properties. However, the issues of oxygen nonstoichiometry of SF and partial molar thermodynamics of oxygen are closely related to the defect structure. This complex subject is fully addressed in another study [21]. For the purpose of the present work and in order to point up existing disagreements, it would be sufficient to say that Δh_O ranges from -65 to -110 kJ/mol O depending on particular data set used for its evaluation [21].

Thereby, in this study we aimed to address the lack of high-temperature thermodynamic data for cubic SF by measuring its enthalpy increments in the broad temperature range (373–1273 K) in air atmosphere and to discuss the oxygen exchange energetics for cubic SF on the basis of the as-obtained in situ calorimetric data.

Results and discussion

Phase transition in SF in air

It is known from the previous studies that the lattice of SF slowly cooled to room temperature in air is tetragonal ($I4/mmm$), and that it undergoes first-order phase transition to cubic ($Pm\bar{3}m$) upon heating in air [1, 4, 9]. The latent heat of this phase transition, ΔH^0_{tr}, should be taken into account in the present discussion of drop calorimetry results. In order to verify the temperature of $I4/mmm \rightarrow Pm\bar{3}m$ phase transition independently, dilatometry experiment was carried out. As seen in Fig. 1, the onset of the peak on thermal expansion coefficient (TEC) dependence is observed at around 548 K. It is in good agreement with some of the earlier reported phase transformation temperatures, T_{tr}, 558 K[4] and 560 K [9]. Though, according to Takeda et al. [1], the said phase transition occurs at slightly lower temperature (523 K), we suppose that direct heat capacity measurements [9] should be given higher priority in correct T_{tr} determination. Thus, at 523 K SF sample in equilibrium with ambient air apparently possesses tetragonal symmetry. In accordance with our in situ X-ray diffraction (XRD) experiment and structural studies of Schmidt and Campbell [4], cubic SF is stable in air at temperatures of 573 K and higher.

Enthalpy increments

During the drop calorimetric experiments, we obtained some values of $\Delta^{T\ high}_{T\ low}H^0$, where T_{low} and T_{high} are the initial and final temperatures of the sample, respectively. As the initial sample temperature, T_{low}, differed slightly from the desired

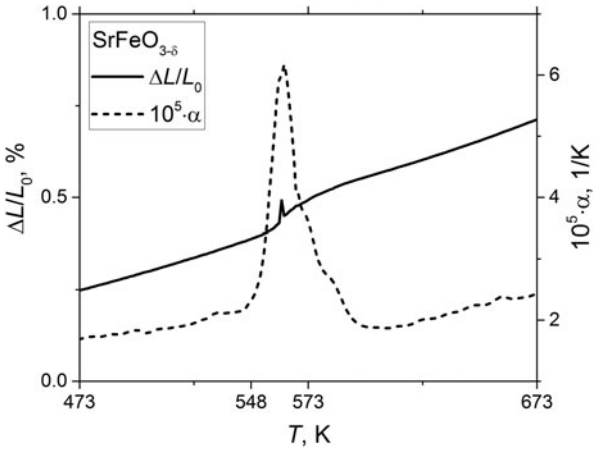


Figure 1: Relative thermal expansion ($\Delta L/L_0$) and TEC (α) of SF in air.

https://doi.org/10.1557/jmr.2019.143 Published online by Cambridge University Press

© Materials Research Society 2019

298 K (see Experimental for details), our experimental points were adjusted using the following expression:

$$\Delta_{298}^{T}H^{0} = \Delta_{T\ \mathrm{low}}^{T\ \mathrm{high}}H^{0} + \Delta_{298}^{T\ \mathrm{low}}H^{0} = \Delta_{T\ \mathrm{low}}^{T\ \mathrm{high}}H^{0} + \int_{298}^{T\ \mathrm{low}} C_{p}^{\mathrm{tetr}}\mathrm{d}T \quad , \tag{1}$$

where $C_{\mathrm{p}}^{\mathrm{tetr}}(T)$ dependence was obtained using the near-room-temperature heat capacity data measured by Haavik et al. [11] for $SrFeO_{2.833}$, because the oxygen content, $3-\delta$, in the slowly cooled SF used in the present work was found to be 2.82(4), which is almost the same as in the samples used by Haavik et al. [11] for heat capacity measurements. Values of $\Delta_{298}^{T}H^{0}$ calculated accordingly are presented in Fig. 2 with the corresponding error margins, and are listed along with experimental data in Table I.

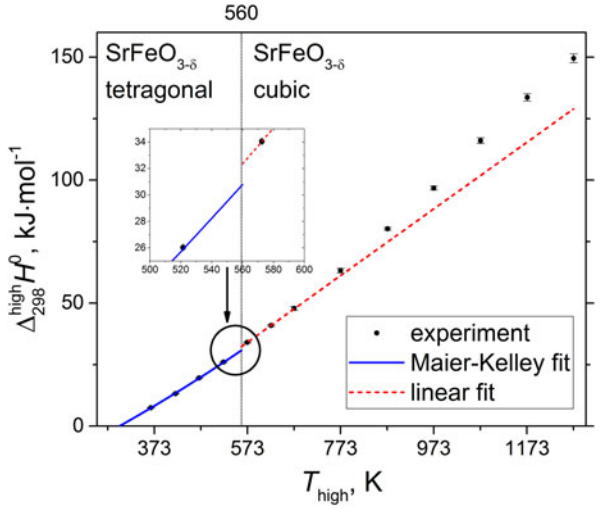


Figure 2: Enthalpy increments for SF: experimental data points and smoothed lines.

TABLE I: Experimental enthalpy increments $\Delta_{T\ \mathrm{low}}^{T\ \mathrm{high}}H^{0}$ and $\Delta_{298}^{T}H^{0}$. Expanded uncertainties reported correspond to a level of confidence of ca 95%. Estimated expanded uncertainties of T_{low} and T_{high} determination are 0.2 K.

T_{low}, K	T_{high}, K	$\Delta_{T\ \mathrm{low}}^{T\ \mathrm{high}}H^{0}$, kJ/mol	$\Delta_{298}^{T}H^{0}$,[a] kJ/mol	Expanded uncertainty, kJ/mol
300.8	1273.6	149.20	149.48	1.80
299.6	1173.6	133.43	133.59	1.50
298.1	1073.4	116.05	116.04	1.10
298.0	972.9	96.77	96.75	0.80
297.2	873.9	80.29	80.19	0.60
297.3	772.9	63.32	63.22	0.96
295.4	673.0	48.10	47.80	0.78
295.2	623.8	41.23	40.92	0.40
294.6	572.4	34.43	34.05	0.25
294.7	521.5	26.40	26.03	0.26
294.5	469.5	19.94	19.55	0.19
294.7	418.5	13.56	13.19	0.13
295.0	365.4	7.76	7.42	0.08

[a]calculated using $\Delta_{T\ \mathrm{low}}^{T\ \mathrm{high}}H^{0}$ and the low-temperature C_{p} data reported by Haavik et al. [11].

Let us first discuss the lower-temperature region, $T \leq 523$ K, where the heat consumed by the SF sample during the drop experiment is determined solely by the heat capacity of tetragonal SF:

$$\Delta_{298}^{T}H^{0} = \Delta_{298}^{T}H_{\mathrm{tetr}}^{0} = \int_{298}^{T} C_{\mathrm{p}}^{\mathrm{tetr}}\mathrm{d}T \quad . \tag{2}$$

Note that at such low temperatures the oxygen exchange can be safely neglected (see section "Oxygen nonstoichiometry and redox thermodynamics" for details). Then, a simple Maier–Kelley function

$$\Delta_{298}^{T}H^{0} = aT + bT^{2} + cT^{-1} + d \quad , \tag{3}$$

can be used to approximate the enthalpy increments for tetragonal SF. The heat capacity data available [11] and the application of Shomate method [22] allow reducing the number of unknowns in Eq. (3):

$$\begin{cases} a = C_{\mathrm{p}} - 596.3b + c/298.15^{2} \\ d = -298.15a - 298.15^{2}b - c/298.15 \end{cases} , \tag{4}$$

where $C_{\mathrm{p}}(298.15) = 106.47$ J/(mol K) [11]. Substitution of Eq. (4) into Eq. (3) yields $\Delta_{298}^{T}H^{0}(b,c,T)$ function, which was fitted to the experimental enthalpy increments of SF at $T \leq 523$ K. It was found that fixing the value of c coefficient as 0 influences the goodness of fit insignificantly while leaving the only unknown (b) in the model function. Consequently, the value of b obtained as a result of the nonlinear fitting is $(4.23 \pm 0.89)\cdot 10^{-2}$ J/(mol K^2), and the enthalpy increments for tetragonal SF can be determined using the following expression

$$\Delta_{298}^{T}H^{0}(\mathrm{J/mol}) = -27983.32 + 81.24305 \cdot T + 0.0423058 \cdot T^{2} \quad . \tag{5}$$

It should be emphasized that, in order to avoid the rounding errors, increased number of significant digits for coefficients is presented in Eq. (5).

Eq. (5) is plotted in Fig. 2 along with the experimental enthalpy increments, showing the good coincidence between fitted function and experimental points. Additionally, $C_{\mathrm{p}}(T)$ dependence for tetragonal SF, calculated by differentiating Eq. (5), is presented in Fig. 3 alongside the experimental data, measured by Haavik et al. [11] As seen, there is a perfect agreement between the two experimental heat capacity dependences.

In contrast with the lower-temperature region, at $T \geq 573$ K the enthalpy increments have several contributions:

$$\Delta_{298}^{T}H^{0} = \Delta_{298}^{T\ \mathrm{tr}}H_{\mathrm{tetr}}^{0} + \Delta H_{\mathrm{tr}}^{0} + \Delta_{T\ \mathrm{tr}}^{T}H_{\mathrm{cub}}^{0} + \Delta H_{\mathrm{red}}^{0} \cdot \Delta\delta \quad , \tag{6}$$

namely, the low-temperature enthalpy increment $\Delta_{298}^{T\ \mathrm{tr}}H_{\mathrm{tetr}}^{0}$, the latent heat of $I4/mmm \rightarrow Pm\bar{3}m$ phase transformation $\Delta H_{\mathrm{tr}}^{0}$,

https://doi.org/10.1557/jmr.2019.143 Published online by Cambridge University Press

© Materials Research Society 2019

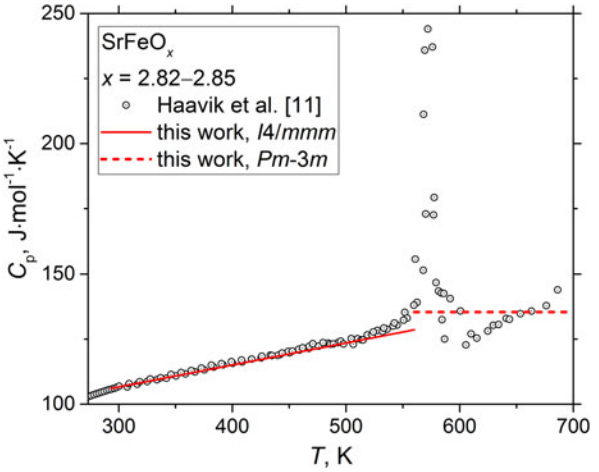


Figure 3: Specific heat of SF: points—data of Haavik et al. [11], line calculated using Maier–Kelley function Eq. (5).

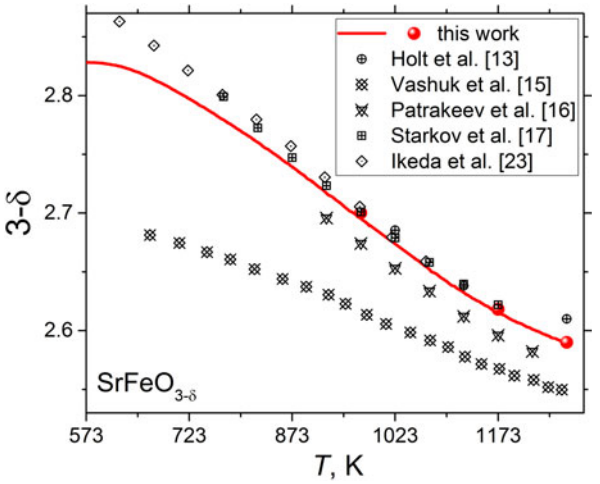


Figure 4: Oxygen content in SF in air as a function of temperature: line—dynamic experiment, points—static measurements.

the "pure" (i.e., without the oxygen exchange contribution) enthalpy increment for cubic SF $\Delta^T_{T\,\mathrm{tr}}H^0_{\mathrm{cub}} = \int_{T\,\mathrm{tr}}^{T} C_{\mathrm{p}}^{\mathrm{cub}}\mathrm{d}T$, and the reduction enthalpy per mole of oxygen atoms $\Delta H^0_{\mathrm{red}}$, multiplied by the change in oxygen stoichiometry during the sample heating $\Delta\delta$. As the oxygen nonstoichiometry in SF changes significantly upon heating at high temperatures, the last term in Eq. (6) cannot be ignored outright. Besides, the knowledge of $\Delta\delta(T)$ dependence is required for the correct experimental data evaluation.

Oxygen nonstoichiometry and redox thermodynamics

The oxygen nonstoichiometry of SF in air is presented in Fig. 4, where solid line was obtained as a result of a dynamic TG experiment in a slow cooling mode (100 K/h), in comparison with the literature data. It can be seen in Fig. 4 that almost no oxygen exchange occurs up to around 623 K. The lower-temperature ($T < 873$ K) discrepancies between the oxygen content curve measured in dynamic mode in the present work and the data of Ikeda et al. [23] and Starkov et al. [17] may be caused by some kinetic limitations at such low temperatures. However, most of the $\delta(T)$ data, both our and those reported in literature [13, 17, 23], agree with each other quite well at $T \geq 873$ K, with maximum discrepancies up to $\Delta\delta = 0.01$. While the shape of the $\delta(T)$ dependence measured by Patrakeev et al. [16] is similar, the absolute δ values exceed those of others by around 0.02. Presumably, it can be attributed to the differences in the absolute reference δ values used by Patrakeev et al. [16] and the others. Indeed, the difficulties in the absolute δ determination for SF were pointed out earlier [7]. Interestingly, the data reported by Vashuk et al. [15] differ strongly from those of others [13, 16, 17, 23] both in shape and values. Therefore, we have to assume some experimental error on their part.

In course of the drop calorimetric experiment $SrFeO_{2.82(4)}$ sample loses oxygen, attaining the oxygen content of $(2.82(4) - \Delta\delta)$. Even at temperature as high as 673 K, where $\Delta\delta \cong 0.01$, the total heat effect associated with the oxygen exchange, $\Delta H^0_{\mathrm{red}} \cdot \Delta\delta$, is expected to be less than the measurement uncertainty. Therefore, for the purpose of calorimetric data evaluation, we can treat the enthalpy increments for SF between 573 and 673 K as belonging to the constant-composition sample. Assuming that high-temperature C_{p} of SF is nearly constant, a linear fit, the results of which are plotted as dashed red line in Fig. 2, was used to estimate a trend in the high-temperature enthalpy increments of cubic SF with constant composition:

$$\Delta^T_{298}H^0_{\delta=0.18}(\mathrm{J/mol}) = \Delta^T_{298}H^0 - \Delta H^0_{\mathrm{red}} \cdot \Delta\delta = -43497 + 135.44\Delta T \quad . \tag{7}$$

In the inset in Fig. 2, the magnified plot of $\Delta^T_{298}H^0(T)$ dependence around the temperature of $I4/mmm \rightarrow Pm\bar{3}m$ phase transition is shown. A very small but distinct vertical gap is seen between the $\Delta^T_{298}H^0(T)$ functions for tetragonal [Eq. (5)] and cubic [Eq. (7)] SF at the phase transformation temperature. This gap corresponds to the phase transition enthalpy ΔH^0_{tr}, the value of which can be found by subtracting Eq. (5) from Eq. (7) assuming $T = T_{\mathrm{tr}} = 560$ K (see section "Phase transition in SF in air" for the discussion of T_{tr}). As-calculated in the present work $\Delta H^0_{\mathrm{tr}} = 1.57$ kJ/mol is close to the value of 2.07 kJ/mol reported by Haavik et al. [9], especially taking into account corresponding uncertainties that, however, are hard to estimate in both cases.

Extrapolated to higher temperatures linear dependence $\Delta^T_{298}H^0_{\delta=\mathrm{const}}(T)$, expressed by Eq. (7), can be subtracted from the experimental enthalpy increments and then divided by the corresponding $\Delta\delta$ to calculate the temperature-dependent

https://doi.org/10.1557/jmr.2019.143 Published online by Cambridge University Press

Journal of Materials Research ■ Volume 34 ■ Issue 19 ■ Oct 14, 2019 ■ www.mrs.org/jmr

© Materials Research Society 2019

values of the reduction enthalpy for cubic SF. Obtained accordingly $\Delta H^0_{red}(T)$ points are presented as circles in Fig. 5. The average ΔH^0_{red} value between 873 and 1273 is 76 ± 7 kJ/mol O, which is close to 70 ± 15 kJ/mol O, extrapolated by Cheng et al. [8] (plotted as a gray dashed line in Fig. 5).

The values of ΔH^0_{red} evaluated by Haavik et al. [10] are also shown in Fig. 5. The difference between triangles and squares results from the difference in reported values of $Ibm2 \rightarrow Pm\bar{3}m$ transition enthalpy in $SrFeO_{2.5}$, taken by Haavik et al. [10] for their calculations. Taking into consideration corresponding error margins, our values of ΔH^0_{red} are close to those calculated by Haavik et al. [10] However, the slight downward trend in $\Delta H^0_{red}(T)$ reported by Haavik et al. [10] is not supported by our study, which is likely caused by some of the concerns we raised regarding their methodology (see Introduction).

It is seen in Fig. 5 that at temperatures between 973 and 1073 K a noticeable increase in ΔH^0_{red} occurs, from 65 ± 7 kJ/mol O at 873–973 K to 84 ± 7 kJ/mol O at 1073–1273 K. In this respect, an interesting comparison can be made between calorimetrically determined ΔH^0_{red} and partial molar enthalpies of oxygen evaluated using the equilibrium $p_{O_2} - T - \delta$ data. As it has already been mentioned, these data reported by different authors scatter significantly [10, 21], resulting in the large discrepancies in the Δh_O values. Surprisingly, most of the nonstoichiometry data for SF [2, 7, 16, 18, 19] yield unreasonably high Δh_O—more than 100 kJ/mol O [21]—which clearly falls out of the tolerance interval of ΔH^0_{red} (see Fig. 5). The values of Δh_O which are inside the error margins of ΔH^0_{red} can be calculated using the data of Holt et al. [13], Starkov et al. [17] and Sereda et al. [21] Besides, the nonstoichiometry of SF was measured by Starkov et al. [17] in broad temperature range, which allowed evaluating Δh_O from their data in two separate temperature intervals, 873–973 K and 1073–1173 K. As-computed Δh_O are presented in Fig. 5 as horizontal line segments reflecting the particular temperature ranges of $p_{O_2} - T - \delta$ data used for calculations. It should be mentioned that we do not consider $\Delta h_O(\delta)$ dependence in the present work as Δh_O of SF was found to be nearly independent of composition in broad δ range [7, 10, 21].

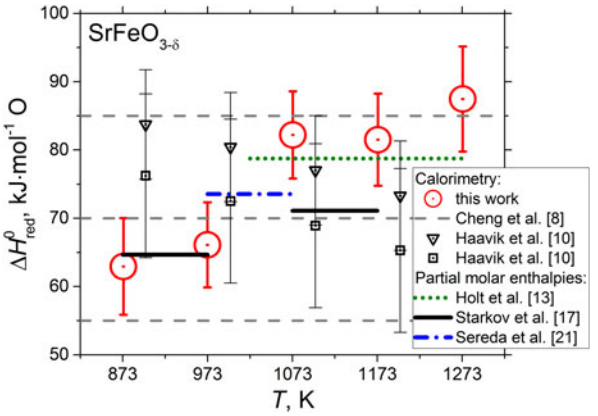


Figure 5: Reduction enthalpies per mol of oxygen atoms for SF, legend explained in the main text.

Notably, the increase in ΔH^0_{red} with temperature, shown in Fig. 5, is evident in both our $\Delta H^0_{red}(T)$ data and, to some extent, in $\Delta h_O(T)$ dependences. It might have been anticipated that, as the increase in temperature causes the expansion of crystal lattice, the Fe–O bond energy should decrease. It should lead to the easing of the oxygen release and result in the decrease in ΔH^0_{red}, which is in apparent contradiction with trends shown in Fig. 5.

In fact, the most plausible explanation of the observed $\Delta H^0_{red}(T)$ dependence can be obtained assuming that not only temperature but some other factors related to the defect chemistry of SF influence its redox energetics. It is known that the charge disproportionation in perovskite-type ferrites is unfavorable, especially when δ is not very close to 0.5 [7, 21, 24], and that various types of the oxygen vacancy ordering are characteristic of undoped strontium ferrite [1, 7, 8, 9, 19, 21]. As it was shown in our previous work [21], even at fairly high temperatures the reduction of SF sample can be described by the single defect reaction

$$2Fe^{\times}_{Fe} + O^{\times}_{O} \rightleftarrows \left(V^{\bullet\bullet}_{O}Fe'_{Fe}\right)^{\bullet} + Fe'_{Fe} + \frac{1}{2}O_2, \qquad K_8 = \frac{\left[Fe'_{Fe}\right]\left[\left(V^{\bullet\bullet}_{O}Fe'_{Fe}\right)^{\bullet}\right]p^{0.5}_{O_2}}{\left[Fe^{\times}_{Fe}\right]^2\left[O^{\times}_{O}\right]}, \quad (8)$$

reflecting the simultaneous oxygen release and the oxygen vacancy cluster formation. The relative charges in reaction (8) correspond to the choice of stoichiometric $SrFeO_3$ as a reference crystal in the Kröger–Vink notation.

In case when the only process (8) is responsible for the SF reduction, ΔH^0_{red} is by definition equivalent to its enthalpy ΔH^0_8. However, the latter is expected to be temperature-independent in broad temperature range because of the linearity of $\ln K_8(1/T)$ dependence [24]. As seen in Fig. 5, ΔH^0_{red} is nearly constant above 1073 K, but not at lower T where it was found to decrease significantly. Consequently, low-temperature defect chemistry of cubic SF should differ from the high-temperature one.

Various degrees of short-range ordering are beneficial for the retaining of the oxygen vacancies [8], and are expected to promote the oxygen vacancy formation (i.e., the reduction) of the oxide, effectively lowering the ΔH^0_{red}. These effects are more prominent at lower temperatures where the ordering processes are less inhibited. In other words, if the ordering in form of the simple vacancy cluster formation expressed as reaction (8) is characteristic of SF at higher temperatures [24], one can expect other types of short-range ordering to arise at lower T resulting in the further decrease in the value of ΔH^0_{red}. And vice versa—

https://doi.org/10.1557/jmr.2019.143 Published online by Cambridge University Press

© Materials Research Society 2019

the increase in temperature should cause the distribution of defects to become more random, making the formation of ordered vacancies energetically less favorable. It results inevitably in the higher values of ΔH^0_{red} at higher temperatures, which is consistent with our observations presented in Fig. 5.

Conclusions

The broad temperature range from 373 to 1273 K in which the enthalpy increments for SF were measured in air atmosphere can be divided into three regions. The lower-temperature region up to the $I4/mmm \rightarrow Pm\bar{3}m$ phase transition temperature of 560 K corresponds to the tetragonal SF which does not release oxygen upon heating. For such constant-composition sample, the simple Maier–Kelley function is adequate for approximating $\Delta^T_{298}H^0(T)$ dependence.

The second region between 573 and 673 K, where SF is cubic, but the oxygen exchange is negligible, was used for estimating the $\Delta^T_{298}H^0(T)$ function for constant-composition SF with $Pm\bar{3}m$ space group.

At even higher temperatures cubic SF loses considerable amount of oxygen upon heating. This process is accompanied by corresponding heat effects, i.e. the reduction enthalpy ΔH^0_{red}. Thus, subtracting $\Delta^T_{298}H^0(T)$ dependence for constant-composition cubic SF from high-temperature enthalpy increments allowed evaluating the ΔH^0_{red} directly from the calorimetric measurements.

The average ΔH^0_{red} value between 873 and 1273 was determined to be 76 ± 7 kJ/mol O, which is close to 70 ± 15 kJ/mol O estimated by Cheng et al. [8] by extrapolating $\Delta H^0_{red}(La_{1-x}Sr_xFeO_{3-\delta}) = f(x)$ dependence. Besides, a pronounced increase in ΔH^0_{red} with temperature, from 65 ± 7 kJ/mol O at 873–973 K to 84 ± 7 kJ/mol O at 1073–1273 K, should be mentioned. The overall tendency of ΔH^0_{red} to increase with T was corroborated by observing the similar behavior of partial molar enthalpies of oxygen, calculated from equilibrium oxygen partial pressure–composition–temperature data reported for SF earlier [13, 17, 21]. Such trend in ΔH^0_{red} of SF was presumed to be caused by the temperature acting as a "disordering force," making the reduction of the sample accompanied by the formation of short-range ordered oxygen vacancies energetically less favorable.

Experimental procedures

Powdered samples of SF were prepared using the glycerol-nitrate technique. A stoichiometric mixture of high-purity $SrCO_3$ and $Fe(C_2O_4)\cdot 2H_2O$ was dissolved in nitric acid. Then a slight excess of glycerol was added, and the resulting solution was heated on a hot plate until the complete evaporation of water followed by self-combustion occurred. Resulting ash was sintered in air at 1073–1373 K for 12 h with intermediate regrindings. X-ray diffraction (XRD) with XRD 7000S (Shimadzu, Kyoto, Japan) using Cu K_α radiation showed that the as-prepared SF powder was single-phase. The exact chemical composition of the SF sample was verified by the inductive coupled plasma (ICP) spectrometer ICAP 6500 DUO and the atomic absorption spectrometer (AAS) Solaar M6 (Thermo Scientific, Waltham, Massachusetts). Chemical compounds used in this work and their estimated purity are listed in Table II.

For calorimetric measurements, small dense pieces of SF were obtained by shattering the SF ceramic pellet, which had been uniaxially pressed and then calcined in air at 1473 K for 12 h. Rectangular bar used for the dilatometry measurements was cut from the as-prepared pellet.

Oxygen content in SF as a function of temperature in air was measured by thermogravimetric technique (TG) using DynTHERM LP ST (Rubotherm, Bochum, Germany) thermobalances. Absolute oxygen content was determined by the sample reduction in the TG setup in a flow of H_2 at 1273 K. Both experimental techniques are described in detail elsewhere [25].

In order to determine the phase transition temperature, dilatometric measurements with DIL 402 C (Netzsch, Selb, Germany) and in situ XRD using XRD 7000S (Shimadzu, Japan), the latter equipped with HTK 1200N (Anton Paar, Graz, Austria) high-temperature oven, were employed. Dilatometric experiment was performed with 2 K/min heating/cooling rate, and during XRD measurements the sample was equilibrated at a target temperature for at least 12 h [25].

An MHTC 96 (Setaram, Lyon, France) drop calorimeter was used for the enthalpy increments' measurements. Sample pieces and small cylinders of reference material (NIST SRM720 monocrystalline sapphire) were alternately dropped from the autosampler at low temperature, T_{low}, to the calorimetric cell, which had been pre-heated to the temperature T_{high} in the range 373–1273 K. In that way, corresponding sensitivity coefficients were obtained during each experimental run [26].

Because the radiative heat transfer from the calorimeter oven to the autosampler, influencing the temperature of the latter, is unavoidable, the autosampler temperature was measured using factory-calibrated digital sensors. Almost linear correlation between the oven and autosampler temperature (T_{high} and T_{low}, respectively) was recorded. T_{low} was found to

TABLE II: Chemical compounds used in the present work.

Chemical name	Source	Mass fraction purity	Analysis method
$SrCO_3$	Vekton	>0.999999	...
$Fe(C_2O_4)\cdot 2H_2O$	Vekton	>0.992	...
HNO_3	Vekton	>0.999999	...
Glycerol ($C_3H_8O_3$)	Khimreaktivsnab	>0.993	...
Sapphire (α-Al_2O_3)	Setaram	>0.9995	...
$SrFeO_{3-\delta}$	Synthesis	>0.99	XRD, AAS

https://doi.org/10.1557/jmr.2019.143 Published online by Cambridge University Press

© Materials Research Society 2019

vary from 294 to 301 K depending on T_{high}, whereas the ambient room temperature was held at around 293 K.

At least 10 drops of both sample and reference were made at each temperature. The reproducibility was found to be within 2.5% even at lowest temperature where the scatter in the increments measured is expected to be the worst. The overall accuracy of the values measured is expected to be ±3%.

In order to return the nonstoichiometry of SF to its initial state, the samples were slowly (100 K per h) cooled along with the calorimetric cell after each experimental run.

All calorimetric and thermogravimetric measurements were performed in ambient air ($p_{O_2} = 0.21$ atm) with average atmospheric pressure 1015 ± 5 mbar.

Acknowledgments

Authors are grateful for financial support to Russian Foundation for Basic Research (RFBR grant No. 18-33-20243\18) and to the Ministry of Education and Science of Russian Federation (State Task No. 4.2288.2017/PCh).

References

1. **Y. Takeda, K. Kanno, T. Takada, O. Yamamoto, M. Takano, N. Nakayama, and Y. Bando**: Phase relation in the oxygen nonstoichiometric system, $SrFeO_x$ ($2.5 \leq x \leq 3.0$). *J. Solid State Chem.* **63**, 237 (1986).
2. **J. Mizusaki, M. Okayasu, S. Yamauchi, and K. Fueki**: Nonstoichiometry and phase relationship of the $SrFeO_{2.5}$–$SrFeO_3$ system at high temperature. *J. Solid State Chem.* **99**, 166 (1992).
3. **J.P. Hodges, S. Short, J.D. Jorgensen, X. Xiong, B. Dabrowski, S. M. Mini, and C.W. Kimball**: Evolution of oxygen-vacancy ordered crystal structures in the perovskite series $Sr_nFe_nO_{3n-1}$ (n = 2, 4, 8, and ∞), and the relationship to electronic and magnetic properties. *J. Solid State Chem.* **151**, 190 (2000).
4. **M. Schmidt and S.J. Campbell**: In situ neutron diffraction study (300–1273 K) of non-stoichiometric strontium ferrite $SrFeO_x$. *J. Phys. Chem. Solids* **63**, 2085 (2002).
5. **A.J. Jacobson**: Materials for solid oxide fuel cells. *Chem. Mater.* **22**, 660 (2010).
6. **J. Sunarso, S. Baumann, J.M. Serra, W.A. Meulenberg, S. Liu, Y. S. Lin, and J.C. Diniz da Costa**: Mixed ionic–electronic conducting (MIEC) ceramic-based membranes for oxygen separation. *J. Membr. Sci.* **320**, 13 (2008).
7. **E. Bakken, S. Stølen, T. Norby, R. Glenne, and M. Budd**: Redox energetics of $SrFeO_{3-\delta}$—A coulometric titration study. *Solid State Ionics* **167**, 367 (2004).
8. **J. Cheng, A. Navrotsky, X-D. Zhou, and H.U. Anderson**: Thermochemistry of $La_{1-x}Sr_xFeO_{3-\delta}$ solid solutions ($0.0 \leq x \leq 1.0$, $0.0 \leq \delta \leq 0.5$). *Chem. Mater.* **17**, 2197 (2005).
9. **C. Haavik, T. Atake, H. Kawaji, and S. Stølen**: On the entropic contribution to the redox energetics of $SrFeO_{3-\delta}$. *Phys. Chem. Chem. Phys.* **3**, 3863 (2001).
10. **C. Haavik, T. Atake, and S. Stølen**: On the enthalpic contribution to the redox energetics of $SrFeO_{3-\delta}$. *Phys. Chem. Chem. Phys.* **4**, 1082 (2002).
11. **C. Haavik, E. Bakken, T. Norby, S. Stølen, T. Atake, and T. Tojo**: Heat capacity of $SrFeO_{3-\delta}$; δ = 0.50, 0.25 and 0.15—Configurational entropy of structural entities in grossly non-stoichiometric oxides. *Dalton Trans.* **3**, 361 (2003).
12. **T. Jia, Z. Zeng, H.Q. Lin, Y. Duan, and P. Ohodnicki**: First-principles study on the electronic, optical and thermodynamic properties of ABO_3 (A = La,Sr, B = Fe,Co) perovskites. *RSC Adv.* **7**, 38798 (2017).
13. **A. Holt, T. Norby, and R. Glenne**: Defects and transport in $SrFe_{1-x}Co_xO_{3-\delta}$. *Ionics* **5**, 434 (1999).
14. **S. Diethelm, A. Closset, J. Van Herle, and K. Nisancioglu**: Oxygen transport and nonstoichiometry in $SrFeO_{3-\delta}$. *Electrochemistry* **68**, 444 (2000).
15. **V.V. Vashuk, L.V. Kokhanovskii, and I.I. Yushkevich**: Electrical conductivity and oxygen stoichiometry of $SrFeO_{3-\delta}$. *Inorg. Mater.* **36**, 79 (2000).
16. **M.V. Patrakeev, J.A. Shilova, E.B. Mitberg, A.A. Lakhtin, I. A. Leonidov, and V.L. Kozhevnikov**: Oxygen intercalation in strontium ferrite: Evolution of thermodynamics and electron transport properties. In *New Trends in Intercalation Compounds for Energy Storage*, C. Julien, J.P. Pereira-Ramos, and A. Momchilov, eds. (Springer, Dordrecht, The Netherlands, 2002); p. 565.
17. **I. Starkov, S. Bychkov, A. Matvienko, and A. Nemudry**: Oxygen release technique as a method for the determination of "δ–pO_2–T" diagrams for MIEC oxides. *Phys. Chem. Chem. Phys.* **16**, 5527 (2014).
18. **O.V. Merkulov, E.N. Naumovich, M.V. Patrakeev, A.A. Markov, H.J.M. Bouwmeester, I.A. Leonidov, and V.L. Kozhevnikov**: Oxygen nonstoichiometry and defect chemistry of perovskite-structured $SrFe_{1-x}Mo_xO_{3-\delta}$ solid solutions. *Solid State Ionics* **292**, 116 (2016).
19. **J. Yoo, C-Y. Yoo, J-H. Yu, and A.J. Jacobson**: Determination of oxygen nonstoichiometry in $SrFeO_{3-\delta}$ by solid-state Coulometric titration. *J. Am. Ceram. Soc.* **100**, 2690 (2017).
20. **J. Vieten, B. Bulfin, M. Senholdt, M. Roeb, C. Sattler, and M. Schmücker**: Redox thermodynamics and phase composition in the system $SrFeO_{3-\delta}$–$SrMnO_{3-\delta}$. *Solid State Ionics* **308**, 149 (2017).
21. **V.V. Sereda, D.S. Tsvetkov, I.L. Ivanov, and A.Y. Zuev**: Interplay between chemical strain, defects and ordering in $Sr_{1-x}La_xFeO_3$ materials. *Acta Mater.* **162**, 33 (2019).
22. **C.H. Shomate**: A method for evaluating and correlating thermodynamic data. *J. Phys. Chem.* **58**, 368 (1954).
23. **H. Ikeda, S. Nikata, E. Hirakawa, A. Tsuchida, and N. Miura**: Oxygen sorption/desorption behavior and crystal structural change for $SrFeO_{3-\delta}$. *Chem. Eng. Sci.* **147**, 166 (2016).

https://doi.org/10.1557/jmr.2019.143 Published online by Cambridge University Press

© Materials Research Society 2019

24. **J. Mizusaki, M. Yoshihiro, S. Yamauchi, and K. Fueki**: Nonstoichiometry and defect structure of the perovskite-type oxides $La_{1-x}Sr_xFeO_{3-d}$. *J. Solid State Chem.* **58**, 257 (1985).
25. **A.Y. Zuev and D.S. Tsvetkov**: Conventional methods for measurements of chemo-mechanical coupling. In *Electro-Chemo-Mechanics of Solids*, S.R. Bishop, N.H. Perry, D. Marrocchelli, and B.W. Sheldon, eds. (Springer International Publishing, Cham, Switzerland, 2017); p. 5.
26. **V.V. Sereda, D.S. Tsvetkov, A.L. Sednev, A.I. Druzhinina, D. A. Malyshkin, and A.Y. Zuev**: Thermodynamics of Sr_2NiMoO_6 and Sr_2CoMoO_6 and their stability under reducing conditions. *Phys. Chem. Chem. Phys.* **20**, 20108 (2018).

https://doi.org/10.1557/jmr.2019.143 Published online by Cambridge University Press

© Materials Research Society 2019